



**HAL**  
open science

## The interplay of hydraulic failure and cell vitality explains tree capacity to recover from drought.

Marylou Mantova, Paulo Eduardo Menezes-Silva, Eric Badel, Hervé Cochard,  
Jose Manuel Torres Ruiz

► **To cite this version:**

Marylou Mantova, Paulo Eduardo Menezes-Silva, Eric Badel, Hervé Cochard, Jose Manuel Torres Ruiz. The interplay of hydraulic failure and cell vitality explains tree capacity to recover from drought.. *Physiologia Plantarum*, inPress, 172 (1), pp.247-257. 10.1111/ppl.13331 . hal-03109304

**HAL Id: hal-03109304**

**<https://hal.inrae.fr/hal-03109304>**

Submitted on 26 Apr 2021

**HAL** is a multi-disciplinary open access archive for the deposit and dissemination of scientific research documents, whether they are published or not. The documents may come from teaching and research institutions in France or abroad, or from public or private research centers.

L'archive ouverte pluridisciplinaire **HAL**, est destinée au dépôt et à la diffusion de documents scientifiques de niveau recherche, publiés ou non, émanant des établissements d'enseignement et de recherche français ou étrangers, des laboratoires publics ou privés.



Physiologia Plantarum

**The interplay of hydraulic failure and cell vitality explains tree capacity to recover from drought**

Journal:	<i>Physiologia Plantarum</i>
Manuscript ID	PPL-2020-00725.R1
Manuscript Type:	Regular manuscript - Ecophysiology, stress and adaptation
Date Submitted by the Author:	n/a
Complete List of Authors:	Mantova, Marylou; INRAE- University Clermont Auvergne Menezes Silva, Paulo; Instituto Federal de Educação Ciência e Tecnologia Goiano - Campus Rio Verde, Department of biology Badel, Eric; INRAE - University Clermont Auvergne Cochard, Hervé; INRA Centre Clermont-Ferrand-Theix-Lyon Torres-Ruiz, José M.; INRAE - University Clermont Auvergne, PIAF
Key Words:	cavitation, drought, tree mortality, cell death, Plant Hydraulics

SCHOLARONE™  
Manuscripts

1  
2  
3 1 **The interplay of hydraulic failure and cell vitality explains tree capacity to**  
4 **recover from drought**  
5  
6  
7  
8  
9

10 4 Marylou Mantova<sup>1</sup>, Paulo E. Menezes-Silva<sup>2</sup>, Eric Badel<sup>1</sup>, Hervé Cochard<sup>1</sup>, José M. Torres-  
11 Ruiz<sup>1,\*</sup>  
12  
13  
14  
15

16 7 <sup>1</sup>Université Clermont Auvergne, INRAE, PIAF, 63000 Clermont-Ferrand, France  
17

18 8 <sup>2</sup>Laboratório de Fisiologia Vegetal, Instituto Federal de Educação, Ciência e Tecnologia Goiano, IF  
19 Goiano, 75901970 Rio Verde, Brasil  
20  
21

22 10

23  
24  
25 11 **Correspondence**

26  
27 12 \*Corresponding author,  
28

29 13 e-mail : torresruizjm@gmail.com  
30  
31  
32  
33  
34  
35  
36  
37  
38  
39  
40  
41  
42  
43  
44  
45  
46  
47  
48  
49  
50  
51  
52  
53  
54  
55  
56  
57  
58  
59  
60

1  
2  
3 15 **Abstract**  
4

5 16 Global climatic models predict an increment in the frequency and intensity of drought events, which  
6 17 have important consequences on forest dieback. However, the mechanisms leading to tree mortality  
7 18 under drought conditions and the physiological thresholds for recovery are not totally understood yet.  
8 19 This study aimed to identify what are the key physiological traits that determine the tree capacity to  
9 20 recover from drought. Individuals of a conifer (*Pseudotsuga menziesii* M.) and an angiosperm (*Prunus*  
10 21 *lusitanica* L.) species were exposed to drought and their ability to recover after rehydration monitored.  
11 22 Results showed that the actual thresholds used for recovery from drought based on percentage loss of  
12 23 conductance (PLC) (i.e. 50% for conifers, 88% for angiosperms) do not provide accurate insights about  
13 24 the tree capacity for surviving extreme drought events. On the contrary, differences in stem relative  
14 25 water content (RWC<sub>Stem</sub>) and the level of electrolytes leakage (EL) were directly related to the capacity  
15 26 of the trees to recover from drought. This was the case for the conifer species, *P. menziesii*, for which  
16 27 higher RWC<sub>Stem</sub> and lower EL values were related to the recovery capacity. Even if results showed a  
17 28 similar trend for the angiosperm *P. lusitanica* as for the conifers, differences between the two traits were  
18 29 much more subtle and did not allow an accurate differentiation between trees able to recover and those  
19 30 that were not. RWC<sub>Stem</sub> and EL could work as indicators of tree capacity to recover from drought for  
20 31 conifers but more studies are required to confirm this observation for angiosperms.  
21  
22  
23  
24  
25  
26  
27  
28  
29  
30  
31  
32

## 33 Introduction

34 Forests represent ca. 30% of the global continental surface (FAO 2006) and provide society with  
35 several ecosystem services such as timber production, watershed protection (Allen et al. 2010), hosting  
36 biodiversity (Trumbore et al. 2015), and carbon storage and its associated atmospheric feedbacks  
37 (Reichstein et al. 2013). Due to the ongoing climate changes and global warming (IPCC 2014), not only  
38 the frequency of heatwaves and drought events have increased in many areas worldwide but also their  
39 duration and intensity (Allen et al. 2010). A recent data synthesis has suggested that the majority of  
40 plant species converge to narrow hydraulic safety margins and thus are very susceptible to changes in  
41 rainfall patterns (Choat et al. 2018). Therefore, these higher frequencies and increased severity have  
42 exacerbated the occurrence of drought-induced tree mortality events (Keenan et al. 2013, Duan et al.  
43 2014) and, consequently, forests dieback (Hosking and Hutcheson 1988, Lwanga 2003, Landmann and  
44 Dreyer 2006).

45 Although the reduction in water availability can affect virtually all processes associated with  
46 plant growth and development, drought-induced tree mortality events are commonly associated with  
47 two main processes: carbon starvation and xylem hydraulic failure (McDowell et al. 2008). Under  
48 prolonged mild drought conditions, trees partially close their stomata to reduce evapotranspiration and  
49 hence the risk of xylem hydraulic failure. However, this stomatal closure constrains CO<sub>2</sub> diffusion in  
50 leaves and can lead to an important depletion of the carbohydrate pools resulting in carbon starvation  
51 (Hogg and Hurdle 1997, Buckley 2005, McDowell et al. 2008, Berry et al. 2010, Creek et al. 2020).  
52 Even if carbon starvation and xylem hydraulic failure cannot be considered as mutually exclusive  
53 processes, recent studies have shown that xylem hydraulic failure is the main cause of tree mortality  
54 under severe drought (Urli et al. 2013, Salmon et al. 2015, Adams et al. 2017). Xylem hydraulic failure  
55 occurs when the tension in the continuous columns of water that connect the roots with the leaves  
56 through the xylem increases and, consequently, exacerbates the risk of cavitation (breakage of the water  
57 column) (Tyree and Zimmermann 2002). This process is widely amplified as soil dries or when the  
58 evaporative demand increases. Thus, under extreme drought conditions, as the percentage of cavitating  
59 conduits increases, the hydraulic conductance of the xylem decreases until the flow of water stops and  
60 provokes the desiccation of the plant tissues, cells death and, finally, the death of the tree (McDowell et  
61 al. 2008). This makes xylem vulnerability to cavitation one of the main physiological traits when  
62 evaluating drought-induced mortality.

63 Even if the vulnerability to cavitation has been widely evaluated for an important amount of  
64 species during the last decades (Delzon et al. 2010, Choat et al. 2012), the relationship between xylem  
65 hydraulic failure and tree mortality has not been properly evaluated yet. It is known that  $P_{50}$  and  $P_{88}$  (i.e.  
66 the xylem tension inducing 50 and 88% of loss of hydraulic conductance, respectively) are associated  
67 with the capacity of the trees to recover from drought (Brodribb et al. 2010, Delzon and Cochard 2014,

1  
2  
3 68 Sperry and Love 2015, Bolte et al. 2016), but the physiological causes of tree death under extreme  
4 69 drought events remain unclear. Therefore, due to a lack of physiological thresholds to properly define  
5 70 tree mortality both during or after a drought episode,  $P_{50}$  and  $P_{88}$  values, for conifers and angiosperms  
6 71 respectively (Brodribb and Cochard 2009; Urli et al. 2013), are currently used as proxies for mortality  
7 72 when e.g. modelling the trees' response to drought (Martin-StPaul et al. 2017). However, a recent study  
8 73 by Hammond et al. (2019) reported that the appropriateness of  $P_{50}$  as an indicator of mortality for  
9 74 conifers should be reconsidered as they defined a lethal threshold at 80% of loss of xylem hydraulic  
10 75 conductivity in loblolly pines (*Pinus taeda* L.). Also, it has recently been reported that branch diameter  
11 76 variations were revealing a point of no recovery in lavender species as plants were not able to recover  
12 77 from drought once their elastic water storage localized in the bark were depleted (Lamacque et al. 2020).  
13 78 These results have raised new questions about the role of xylem hydraulic failure in triggering tree  
14 79 mortality or the minimum hydraulic functioning required for allowing trees to survive and recover from  
15 80 drought.

16 81 The ability of the trees to recover after a drought event seems to be tightly related to their ability  
17 82 to grow new xylem (Brodribb et al. 2010) and this ability must be intrinsically linked to their capacity  
18 83 to maintain key living tissues alive in perennial organs, as the stem, that allow them to regrowth and  
19 84 resprout in favourable conditions. Considering the tenet that xylem hydraulic failure should provoke the  
20 85 complete desiccation of the cells and their consequent death leading to whole plant mortality (McDowell  
21 86 et al. 2008), a focus on plant water status and its consequences on cell vitality seems necessary to  
22 87 understand drought-induced mortality (Guadagno et al. 2017, Martinez-Vilalta et al. 2019). This,  
23 88 therefore, highlights the relevance of relative water content (RWC), a direct measure of the plant water  
24 89 status at cell level, as a potential candidate for assessing drought-induced tree mortality (Martinez-  
25 90 Vilalta et al. 2019, Trueba et al. 2019). In addition, and considering that many studies have evinced how  
26 91 low RWC values are linked to membrane dysfunction in plant cells (Wang et al. 2008, Chaturvedi et al.  
27 92 2014), combining both traits, RWC and membrane dysfunction, would help define physiological  
28 93 thresholds for tree mortality.

29 94 The main objective of this study was to identify other physiological traits than the percentage  
30 95 loss of hydraulic conductance (PLC) that could work as an indicator of the tree capacity to recover from  
31 96 drought. For this, a set of plants of *Prunus lusitanica* L. and *Pseudotsuga menziesii* M., i.e. an  
32 97 angiosperm and a conifer species respectively, were exposed to severe drought conditions and allowed  
33 98 to dehydrate until the induction of important losses in hydraulic functioning. At this point, trees were  
34 99 re-watered to check for the capacity to recover from drought. During the dehydration and the recovery  
35 100 phases, we monitored embolism formation and changes in RWC at the stem and the leaf level. We also  
36 101 monitored changes in stem diameter to check whether trees were able to recover from drought after  
37 102 being re-watered, and assessed the vitality of the stem living tissues. Results also provided us with novel

1  
2  
3 103 information about the causative relationship between PLC and tree mortality and the level of PLC that  
4 104 prevent any recovery from drought in these two species.

## 7 105 **Materials and methods**

### 9 106 *Plant material and experimental setup*

11 107 The experiments were carried out in two species: one angiosperm, *Prunus lusitanica* L. and one  
12 108 conifer, *Pseudotsuga menziesii* M., a shrub and a tree respectively, selected for their contrasted PLC  
13 109 thresholds of drought-induced mortality (i.e.  $P_{88}$  and  $P_{50}$  respectively). For each species, eight young  
14 110 trees were grown under non-limiting water conditions in 5 and 9.2-L pots, respectively, at the INRAE-  
15 111 PIAF research station of Clermont-Ferrand, France (45°57'N, 3°14'E). *P. menziesii* individuals were  
16 112 four years old at the time of the experiment while the *P. lusitanica* were two years old. Two weeks  
17 113 before starting the experiment, all trees were moved to a controlled-environment glasshouse cell and  
18 114 kept under natural light and at a mean temperature of  $17.7 \pm 0.2^\circ\text{C}$  (midday) and  $10.9 \pm 0.1^\circ\text{C}$  (night).  
19 115 During this period, trees were kept well-irrigated (field capacity) by a drip irrigation system controlled  
20 116 by an electronic timer. After the two weeks of acclimation, a sub-set of trees for each species (from four  
21 117 to six individuals) was exposed to progressive dehydration by withholding the irrigation. In order to  
22 118 determine the critical PLC for recovery and because Hammond et al. (2019) reported that conifers were  
23 119 able to recover even beyond  $P_{50}$ , trees were re-watered to field capacity once reaching water potential  
24 120 values corresponding to significant losses in hydraulic functioning according to their vulnerabilities to  
25 121 cavitation (i.e. PLC > 50% for conifers and PLC > 90% for angiosperms). They were then kept well-  
26 122 irrigated in order to check for recovery from drought.

### 27 123 *Vulnerability curves to cavitation*

28 124 Prior to the experiment, the vulnerability to cavitation for the two target species was determined  
29 125 to define when trees should be re-watered according to their PLC level. Thus, two different techniques  
30 126 (i.e. one technique per species), reported as highly comparable by Brodribb et al. (2017), were used  
31 127 according to the xylem characteristics of each species. Thus, for *P. lusitanica*, xylem vulnerability to  
32 128 cavitation was determined by using the recently developed optical method (Brodribb et al. 2017) to  
33 129 avoid possible biased results related with the open-vessel artefact (Torres-Ruiz et al. 2014, 2015, Choat  
34 130 et al. 2016). Indeed, the use of the Cavitron method in this species was not possible due to the length of  
35 131 the xylem conduits that were longer than the diameter of the rotor available (Sergent et al. 2020). For *P.*  
36 132 *menziesii*, vulnerability curves were constructed by using the Cavitron technique (Cochard 2002) which  
37 133 is highly reliable when used to measure species with short conduits such as conifers (Cochard et al.  
38 134 2013, Torres-Ruiz et al. 2017). The use of the optical method was not possible for *P. menziesii* because  
39 135 the conduits at the stem level are so short that the cavitation events are not always detectable.

1  
2  
3 136 Briefly, for *P. lusitanica*, the entire plant was let to dehydrate under lab conditions while a clamp  
4  
5 137 equipped with a camera was installed in the stem of four trees after removing the bark carefully with a  
6  
7 138 razor blade to expose undamaged xylem. To avoid the over desiccation of the exposed xylem area during  
8  
9 139 the  $6.51 \pm 0.52$  days of dehydration, we applied a thin coat of silicone grease. The camera then captured  
10  
11 140 images every five min during the dehydration process while changes in stem water potential ( $\Psi_{\text{stem}}$ , MPa)  
12  
13 141 were continuously monitored using a psychrometer (PSY1, ICT international, Armidale, Australia)  
14  
15 142 installed centrally on the main stem of each plant. The Peltier cooling time was adjusted from 10 s (when  
16  
17 143 the plant was well hydrated) to a maximum of 20 s (as the plant dehydrated) to ensure that sufficient  
18  
19 144 water was condensed onto the thermocouple and then evaporated to produce a stable reading of the wet-  
20  
21 145 bulb depression temperature. To ensure the accuracy of the measurements obtained with the  
22  
23 146 psychrometer, regular  $\Psi_{\text{stem}}$  measurements were carried using a Scholander-type pressure chamber  
24  
25 147 (PMS, Corvallis) in fully developed and healthy leaves previously bagged for at least one hour to prevent  
26  
27 148 transpiration and promote equilibrium with the plant axis (Fig. S1). Image sequences were then analysed  
28  
29 149 manually according to Brodribb et al. (2016, 2017). The percentage of embolised pixels for each image  
30  
31 150 was calculated as the amount of embolised pixels cumulated and the total embolised area of the scanned  
32  
33 151 area. The vulnerability curve was obtained by plotting  $\Psi_{\text{stem}}$  against cumulative embolisms (% of total).

34  
35 152 For *P. menziesii*, xylem vulnerability to cavitation was assessed with the Cavitron technique  
36  
37 153 (Cochard 2002) which uses centrifugal force to increase the water tension in a xylem segment while  
38  
39 154 measuring the decrease in its hydraulic conductance. Thus, five 0.45m-long stem samples from five  
40  
41 155 different well-hydrated trees (i.e. one sample per tree), were debarked to prevent resin contamination  
42  
43 156 and recut under water with a razor blade to a standard length of 0.27m. For constructing the vulnerability  
44  
45 157 curves, the maximum sample conductivity ( $K_{\text{max}}$ ) was measured at low speed and relatively high xylem  
46  
47 158 pressure ( $-0.75$  MPa). The xylem pressure was then decreased stepwise by increasing the rotational  
48  
49 159 velocity and the conductivity ( $K$ ) measured at each pressure step. Each pressure was applied on the  
50  
51 160 sample for two minutes. Sample loss of conductivity (PLC, %) was computed at each pressure as  
52  
53 161 follows:

$$54 \quad 162 \quad PLC = 100 * \left(1 - \frac{K}{K_{\text{max}}}\right) \quad (1)$$

55  
56 163 The resulting curves were fitted according to Pammenter and Vander Willigen equation (1998) and  
57  
58 164 using the R 'fitPLC' package:

$$59 \quad 165 \quad PLC \text{ or Cumulative embolism} = \frac{100}{(1 + e^{(a/25)(P - P_{50})})} \quad (2)$$

60  
61 166 where  $a$  is the slope of the curve at the inflexion point,  $P$  indicates the xylem water potential for the  
62  
63 167 optical method (*P. lusitanica*) or the target pressure reached with the Cavitron (*P. menziesii*), and  $P_{50}$  is



1  
2  
3 168 the  $\Psi_{\text{stem}}$  or pressure value at which 50% of the xylem cavitation events had been observed or at which  
4 169 50% loss of conductivity occurred.

6  
7 170 *Physiological traits*

9 171 During the progressive dehydration imposed to each subset of plants,  $\Psi_{\text{stem}}$  was continuously  
10 172 assessed by using psychrometers (PSY1, ICT international). Thus, one psychrometer per plant in a total  
11 173 of four plants per species was installed at the stem level and covered with aluminium foil to prevent  
12 174 their direct exposure to the sunlight and minimize any effect of external temperature variations  
13 175 (Vandegheuchte et al. 2014). Psychrometers recorded the  $\Psi_{\text{stem}}$  every 30 min. To check the accuracy of  
14 176 the psychrometers, regular  $\Psi_{\text{stem}}$  measurements were carried using a Scholander-type pressure chamber  
15 177 (PMS, Corvallis) in two fully developed and healthy leaves per plant, previously bagged for at least one  
16 178 hour to prevent transpiration and promote equilibrium with the plant axis (Fig. S1).

17 179 Stem diameter variations were monitored continuously by Linear Variable Differential  
18 180 Transformer (LVDT) sensors (one LVDT per plant in eight plants per species) installed before  
19 181 withholding irrigation. The sensor was applied on the stem with glue and was connected to a data logger  
20 182 (Model CR1000, Campbell Scientific LTD) to collect the stem diameter variations (in  $\mu\text{m}$ ) every 10  
21 183 min. By evaluating the dynamics of stem diameter during the dehydration and recovery phases of the  
22 184 experiment, we were able to evaluate the capacity of the trees to recover from drought (Lamacque et al.  
23 185 2020).

24 186 The RWC was measured at stem ( $\text{RWC}_{\text{Stem}}$ ) and leaf level ( $\text{RWC}_{\text{Leaf}}$ ) in all trees before  
25 187 withholding irrigation (Control) and right before re-watering.  $\text{RWC}_{\text{Stem}}$  and  $\text{RWC}_{\text{Leaf}}$  were calculated  
26 188 according to Barrs and Weatherley (1962):

$$27 \text{RWC} = \frac{(FW - DW)}{(TW - DW)} \quad (3),$$

28 190 where FW is the fresh weight measured immediately after sampling; TW is the turgid weight measured  
29 191 after immersing the stem in distilled water for 24 h (for  $\text{RWC}_{\text{Stem}}$ ) or after soaking the leaf petiole for 24  
30 192 h in distilled water (for  $\text{RWC}_{\text{Leaf}}$ ); and DW is the dry weight of the samples after 24 h of drying in an  
31 193 oven at 72°C. All measurements were done using a precision scale (METTLER AE 260, DeltaRange  
32 194 ®) and were performed on three healthy leaves or one to three small stem sections per plant (depending  
33 195 on plant material).

34 196 Once the trees reached water potentials corresponding to a PLC of ca. 88% for *P. lusitanica* and  
35 197 50% for *P. menziesii* according to the vulnerability curves, the PLC was assessed in stems using two  
36 198 different, but comparable, techniques (Cochard 1992, Torres-Ruiz et al. 2014, Choat et al. 2016). For *P.*  
37 199 *lusitanica*, PLC was determined gravimetrically using a xylem embolism meter (XYL'EM, Bronkhorst).  
38 200 For *P. menziesii*, as it was impossible to restore the maximal conductance ( $K_{\text{max}}$ ) due to the permanent

201 aspiration of the pit membrane against the cell walls (Cochard et al. 2013), the PLC was assessed by  
 202 direct observation using X-Ray microtomography (Micro-CT, Nanotom 180 XS; GE) at the PIAF  
 203 laboratory (INRAE) (Cochard et al. 2015). For both techniques, samples were cut progressively  
 204 underwater to prevent artefactual increases in the amount of embolism in the samples (Torres-Ruiz et  
 205 al. 2015).

206 For the XYL'EM, the PLC was evaluated in three stems (sample length ca. 30mm) per  
 207 individual in eight individuals per species. The initial  $K$  ( $K_i$ ) of each segment was determined using a  
 208 filtered (0.22  $\mu\text{m}$ ) 10 mm KCl and 1 mm CaCl<sub>2</sub> perfusion solution made with distilled water (Cochard  
 209 et al. 2009), and applying a pressure head of 8.5 kPa until a steady-state  $K_i$  was attained. In order to  
 210 determine the maximal conductance ( $K_{\text{max}}$ ), samples from *P. lusitanica* were flushed with water at high  
 211 pressure (200 kPa) for 20 minutes to remove all the embolism. PLC was then calculated using the  
 212 following equation:

$$213 \quad PLC = 100 * \left(1 - \frac{K_i}{K_{\text{max}}}\right) (4)$$

214 For Micro-CT, one or two samples per plant were collected, as described for the gravimetric  $K$   
 215 measurements, and immediately immersed in liquid paraffin wax to prevent dehydration during the  
 216 scanning. For each 21-min scan, 1000 images were recorded during the 360° rotation of the sample. The  
 217 X-ray setup was fixed at 70kV and 240 $\mu\text{A}$ . At the end of the experiment, samples were cut 3mm above  
 218 the scanned cross-section, injected with air (0.1MPa) and re-scanned to visualize all the conduits filled  
 219 with air. The amount of PLC was computed by determining the ratio between the amount of cavitated  
 220 conduits in the samples before and after cutting the sample.

### 221 *Cell vitality*

222 Cell vitality was assessed using two different methods: the electrolytes leakage test (EL) (Zhang  
 223 and Willison 1987, Sutinen et al. 1992) and a fluorescein diacetate (FDA) staining process (Widholm  
 224 1972). Cell vitality was assessed in both control and drying trees right before rewatering the latter ones.  
 225 For EL, one to three stem samples per plant (depending on plant material availability) were cut into ten  
 226 2-mm thick slices and immersed in test tubes containing 15mL of pure water. Test tubes were shaken at  
 227 60 shakes per min during 24h at 5°C to stop enzyme activity. Water conductivity of the effusate (C1)  
 228 was then measured at room temperature using a conductimeter (3310 SET1, Tetracon® 325, WTW,  
 229 Weilheim, Germany). Then, all the living cells were killed by autoclaving the samples at 121°C for 30  
 230 min (King and Ludford 1983), cooled down at room temperature (22°C approx.) for 60 min and the  
 231 effusate maximal conductivity (C2) measured. The lysis percentage (EL) was then determined as:

$$232 \quad EL = \frac{C1}{C2} * 100 (5)$$

233 To stain the cytoplasm of stem living cells and quantify the amount of living cells and their  
 234 location for each individual, FDA (F7378-10G, SIGMA-ALDRICH) was used. For this, two or three 60  
 235  $\mu\text{m}$ -thick stem cross-sections were obtained with a microtome (Leica RM2165) and stained for 20 min  
 236 in a 1% FDA solution (Widholm 1972). Cross-sections were observed using an inverted fluorescence  
 237 microscope (Axio Observer Z1, ZEISS; Bright light or YFP filter) within the next hour after staining.  
 238 An entire cross-section image was obtained by joining images with the same magnification taken from  
 239 all the cross-section of the sample for both bright light and fluorescence observations. The percentage  
 240 of bark living cells (BLC) for each cross-section was calculated as follow:

$$BLC = \frac{FA}{BA} * 100 \quad (6)$$

242 Where FA is the total fluorescent area of the sample and BA is the bark area determined using Fiji  
 243 software (Schindelin et al. 2012).

#### 244 *Statistical analyses*

245 Statistical analyses consisted of paired *t*-test (after testing for normality and homogeneity of  
 246 variances) and Wilcoxon test (for non-normal distribution) and were performed using R programs to  
 247 compare the set before the drought event (Control) and before re-watering. All tests were performed  
 248 using a level of significance  $\alpha = 0.05$ .

## 249 **Results**

### 250 *Capacity of recovery from drought*

251 Vulnerability curves reported  $P_{50}$ -values of -6.07 and -3.73MPa for *P. lusitanica* and *P.*  
 252 *menziesii*, respectively (Fig. 1). *P. lusitanica* individuals were thus rehydrated once they reached water  
 253 potential values of ca. -9.0 to -10.0MPa i.e. above its  $P_{88}$  of -8.94MPa. *P. menziesii* were rehydrated  
 254 once showing water potential of ca. -7.0 to -10.0 MPa ( $P_{88} = -5.34\text{MPa}$ ).

255 In control conditions, the mean levels of PLC in the stem for *P. lusitanica* and *P. menziesii* were  
 256 6.9 ( $\pm 3.5$  SE) and 7.40 ( $\pm 2.8$  SE) respectively (Fig. 2). Right before applying the recovery irrigation, the  
 257 mean PLC for *P. lusitanica* and *P. menziesii* were 94.4 ( $\pm 1.98$  SE) and 79.5 ( $\pm 3.7$  SE) respectively  
 258 (Table S1) i.e. above the current point for xylem hydraulic failure for angiosperms (i.e.  $P_{88}$ ) and conifers  
 259 (i.e.  $P_{50}$ ).

260 Stems showed a noticeable shrinkage for both species during the time-course of the dehydration  
 261 for all individuals (Fig. 3). After rewatering, two *P. lusitanica* individuals that reached a mean PLC of  
 262 90.3 ( $\pm 8.3$  SE) (Fig. 2A) showed an increase in stem diameter immediately after being re-hydrated and  
 263 were considered as recovered trees (Fig. 3A). On the contrary, the six individuals that reached PLC of  
 264 95.8 ( $\pm 1.1$  SE) showed a continuous decrease in stem diameter after the rehydration and were considered

265 as dead trees (Fig. 3C). For *P. menziesii*, only one individual that reached a  $\Psi_{\text{stem}}$  value of -7.48MPa and  
 266 a PLC level of 67.9 (Fig. 2B) was able to recover in terms of trunk diameter after rewatering (Fig. 3B).  
 267 All the other individuals continued to show a decrease in stem diameter during the re-watering phase  
 268 after reaching a mean  $\Psi_{\text{stem}}$  value of -8.7MPa ( $\pm 0.5$  SE) (Fig. 3D) and a mean PLC of 81.1 ( $\pm 3.8$  SE)  
 269 (Fig. 2B).

270 For both species, individuals that were able to recover from drought showed an increase in  $\Psi_{\text{stem}}$   
 271 concomitantly to the increase in stem diameter (Fig. 3A, B) while no recovery in  $\Psi_{\text{stem}}$  was noticed in  
 272 trees considered as dead (Fig. 3C and Fig. 3D).

273 A significant decrease in  $\text{RWC}_{\text{Stem}}$  was observed for both species during dehydration as PLC  
 274 increases (Fig. 4A and Fig. 4B; Table S2). In control *P. lusitanica* trees,  $\text{RWC}_{\text{Stem}}$  was of 92.3% ( $\pm 0.8$   
 275 SE) whereas it dropped for those exposed to drought to 58.5% ( $\pm 1.5$  SE) for recovered individuals and  
 276 to 54.7% ( $\pm 3.6$  SE) for dead individuals before re-watering. Differences in  $\text{RWC}_{\text{Stem}}$ , however, were not  
 277 significant when comparing recovered and dead individuals. Similar results were observed for *P.*  
 278 *menziesii*, with a significant decrease in  $\text{RWC}_{\text{Stem}}$  noticed for both recovered and dead individuals from  
 279 drought. Thus,  $\text{RWC}_{\text{Stem}}$  decreased from 83.4% ( $\pm 1.1$  SE) for control trees to 49.8% for recovered and  
 280 36.9% ( $\pm 1.9$  SE) for dead trees.

281 Similar to  $\text{RWC}_{\text{Stem}}$ ,  $\text{RWC}_{\text{Leaf}}$  was significantly impacted in both species during dehydration  
 282 (Fig. 4C, D; Table S2). For *P. lusitanica*,  $\text{RWC}_{\text{Leaf}}$  decreased from 94.8 % ( $\pm 0.5$  SE) (Control) to 56.9%  
 283 ( $\pm 4.1$  SE) in plants that recovered from drought and to 59.3 % ( $\pm 4.8$  SE) in those that did not recover.  
 284 For *P. menziesii*,  $\text{RWC}_{\text{Leaf}}$  went from 92.4 % ( $\pm 2.0$  SE) (Control) to 53.5 % in recovered trees or 51.5  
 285 % ( $\pm 4.7$  SE) in dead trees. Differences in  $\text{RWC}_{\text{Leaf}}$  were not significant for any of the two species when  
 286 comparing recovered and dead individuals.

#### 287 *Tissue vitality*

288 For *P. lusitanica*, all trees showed higher EL values than control ones before re-watering (Fig.  
 289 4E and Fig. 4F, Table S2) (Control: 29.9%  $\pm 1.3$  SE; Recovered: 47.12%  $\pm 7.12$  SE; Dead: 57.2%  $\pm 6.7$   
 290 SE). However, no differences were noticed when comparing recovered and dead individuals before re-  
 291 watering (Recovered: 47.1%  $\pm 7.1$  SE; Dead: 57.2%  $\pm 6.7$  SE). For, *P. menziesii*, only the trees that did  
 292 not recover showed higher EL values compared to control (Control: 50.6%  $\pm 2.2$  SE; Dead: 78.8%  $\pm 2.2$   
 293 SE). No differences in EL were observed between the recovered individual and control ones (Control:  
 294 50.6%  $\pm 2.2$  SE; Recovered: 50.8%). The recovered individual tends to show lower EL values than the  
 295 dead ones (Recovered: 50.8%; Dead: 78.8%  $\pm 1.2$  SE).

296 In control trees and for both species, the FDA staining showed that living cells were mostly  
 297 located at the outer bark and phloem level (Fig. 5). Before re-watering, the amount of living cells in *P.*  
 298 *lusitanica* decreased noticeably in dead trees (Fig. 6A; Table S3) (Control: 23.0%  $\pm 4.4$  SE; Dead: 3.0%

299  $\pm 1.4$  SE) but not in trees that recovered (Control: 23.0%  $\pm 2.4$  SE; Recovered: 15.3%  $\pm 10.4$  SE). For *P.*  
300 *menziesii*, the amount of living cells decreased in trees that did not recover (Control: 10.2%  $\pm 2.1$  SE;  
301 Dead: 0.8%  $\pm 0.6$  SE) while no noticeable decrease was encountered in trees that recovered (Control:  
302 10.2%  $\pm 2.2$  SE; R: 7.2%) (Fig. 6B; Table S3).

## 303 Discussion

304 Our results provide strong evidence that even when presenting high levels of hydraulic  
305 dysfunction, trees were able to recover from an extreme drought event after being re-watered. Indeed,  
306 *P. lusitanica* individuals that showed PLC values of 98.6%, i.e. well above the suggested threshold for  
307 recovery and point of death for angiosperms ( $P_{88}$ , Barigah et al. 2013; Urli et al. 2013), recovered from  
308 drought according to their stem diameter dynamic (i.e. showed an increase in stem diameter immediately  
309 after re-watering) and even flushed new leaves after being re-watered at field capacity (Fig. S2).  
310 Similarly, *P. menziesii* individuals with PLC values of 67.9%, i.e. above the threshold for recovery for  
311 conifers ( $P_{50}$ , Brodribb and Cochard 2009), were also able to recover once re-watered. These results,  
312 therefore, demonstrate how trees are able to recover from drought even when their PLC levels reach  
313 higher values than those considered as threshold for recovery for angiosperms and conifers (i.e.  $P_{88}$  and  
314  $P_{50}$ , respectively). These results agree with those provided for loblolly pine (*Pinus taeda* L.) by  
315 Hammond et al. (2019) which reported a higher chance for trees to die than to survive once reaching  
316 PLC levels of 80, i.e. much higher than the  $P_{50}$  threshold commonly reported for conifers. In our study,  
317 however, no recovery was observed for *P. menziesii* when PLC reached values above 68%, which raises  
318 questions on how lethal PLC thresholds vary among tree species. For angiosperms, our results also agree  
319 with the ones provided for *Pistacia lentiscus* L. by Vilagrosa et al. (2003) that show how drought-  
320 induced mortality only occur in plants that reached PLC values of almost 100%. When taken together,  
321 all these results highlight the importance of revising the actual recovery and point of death thresholds  
322 suggested for angiosperms and conifers. More importantly, these results show that plant mortality occurs  
323 when the losses in xylem conductance are important (e.g. >90% of xylem hydraulic dysfunction),  
324 suggesting that PLC is not the sole triggering mechanism of plant death under drought conditions.

325 Unfortunately, any critical thresholds for most of the physiological traits monitored during our  
326 experiment were identified as a potential proxy for drought-induced mortality. Thus, it was not possible  
327 to evince a clear causal link between stem hydraulic failure and plant mortality since trees that were not  
328 able to recover from drought did not consistently show higher PLC values than those that survived.  
329 However, two interesting trends emerged from the  $RWC_{Stem}$  and EL results for *P. menziesii*. On one  
330 hand, trees recovering from drought tend to show higher  $RWC_{Stem}$  than dead ones before re-watering  
331 and, on the other hand, trees that recovered tend to show lower EL values than the dead ones. These  
332 results agree with Martinez-Vilalta et al. (2019) and highlight the importance of plant water content as  
333 a potential indicator of mortality risk. However, this was not the case for *P. lusitanica* since similar

1  
2  
3 334  $RWC_{Stem}$  values were observed in both trees that were able to recover from drought and those that were  
4 335 not. This raises the possibility of using  $RWC_{Stem}$  as a proxy for mortality across species, although more  
5 336 confirmatory studies should be carried out especially in angiosperms. At leaf level,  $RWC_{Leaf}$  at turgor  
6 337 loss point is relatively high and constant between species (Bartlett et al. 2012), which potentially could  
7 338 make it a useful trait for identifying survival events since noticeable changes in  $RWC_{Leaf}$  would occur  
8 339 at high dehydration level preceding death (Martinez-Vilalta et al. 2019). However, no differences in  
9 340  $RWC_{Leaf}$  were detected in our study between recovering and dead trees before re-watering for any of the  
10 341 two species evaluated probably because, at those levels of water stress, leaves were already hydraulically  
11 342 disconnected from the stems in all the individuals. This would favour a faster dehydration of the leaves  
12 343 in comparison with the stems and, therefore, may partially explain the similarly low values for  $RWC_{Leaf}$ .  
13 344 Therefore, rather than just focusing only on the plant water status, a deeper study on water relocation in  
14 345 trees during drought (Körner 2019) would be required for identifying potential proxies for drought-  
15 346 induced mortality. In fact, a crucial question now is to evaluate if the relocation of water from plant  
16 347 reserves would be enough for keeping key tree tissues hydrated during drought and, therefore, enhancing  
17 348 plant probability of survival after re-watering (Holbrook 1995).

18  
19 349         Regarding cell integrity, recovering trees from drought tend to present lower cell damages than  
20 350 the dead trees before re-watering. *P. menziesii* recovering trees showed seemingly no changes in their  
21 351 percentage of EL even after the drought event. Dead trees, on the contrary, consistently showed higher  
22 352 EL values before re-watering than control trees able to recover in agreement with the results reported  
23 353 by Vilagrosa et al. (2010) for *P. lentiscus*. Even if *P. lusitanica* dead and recovering trees did not show  
24 354 any differences in EL, recovering trees were able to resprout and flush new leaves when the stress was  
25 355 alleviated (Fig. S2). As higher EL values are the consequences of membrane failure and are associated  
26 356 with cell death (Vilagrosa et al. 2010, Guadagno et al. 2017), these observations suggest that the fatal  
27 357 failure at the cellular scale does not occur homogeneously within the stem and this, as shown by Thomas  
28 358 (2013) and Klimešová et al. (2015), allow the resprouting of the plant if the stress is relieved. Therefore,  
29 359 according to our results, the membrane integrity could emerge as a proxy for lack of recovery capacity  
30 360 in conifers since the cell vitality in some of the living tissues at the stem level seems to have a relevant  
31 361 role in drought-induced mortality. However, the link between membrane failure and the loss in stem  
32 362 hydraulic functioning is still unresolved. Indeed, it is still unclear whether the extreme dehydration leads  
33 363 to membrane failure through physical (i.e. cell cavitation, Sakes et al. 2016), collapse and cytorrhysis  
34 364 (Taiz and Zeiger 2006) or only biochemical processes (Suzuki et al. 2012, Wang et al. 2013, Petrov et  
35 365 al. 2015).

36  
37 366         The presence of living cells in stems at the inner bark level was not always related to the survival  
38 367 of the trees after re-watering (i.e. increase in stem diameter). This was the case for *P. lusitanica* where  
39 368 trees showing similar amounts of living cells, differed in their capacity to recover from drought. The  
40 369 presence of living cells in dead trees could be explained by the fact that, under drought conditions, trees

1  
2  
3 370 can rely on their own water reserves (Epila et al. 2017) which could temporally maintain the metabolism  
4 371 of the cell despite being hydraulically disconnected from the roots. However, once the water reserves  
5 372 are depleted, living tissues would ultimately dry and cells would dehydrate and die. Therefore, not only  
6 373 the presence of living cells is required for allowing the plant to recover from drought but also their  
7 374 hydraulic connection with the other plant tissues and organs upstream. Thus, even at stem PLC values  
8 375 near to 100% for angiosperms or well above 50% for conifers, a minimal hydraulic connection between  
9 376 the soil and the living tissues could be enough to recover from drought if plants have access to water.  
10 377 More studies focused on the link between xylem hydraulic functioning, plant capacitance and cell  
11 378 mortality are therefore required to identify what the thresholds for tree survival to drought are.

## 17 379 **Conclusion**

20 380 By combining a living-cell staining process with LVDT sensors and PLC measurements, this  
21 381 study showed that the common thresholds for recovery and point of death considered until now, i.e  $P_{50}$   
22 382 for conifers and  $P_{88}$  for angiosperms, are not accurate enough for assessing and predicting drought-  
23 383 induced tree mortality. Indeed, our results showed that trees with PLC levels of 98.6% for *P. lusitanica*  
24 384 (angiosperm) and 67.9% for *P. menziesii* (conifer) were still able to recover from drought once re-  
25 385 watered. Thus, even if the link between a high level of stem PLC and tree mortality is clear, there is an  
26 386 urgent need in defining new physiological thresholds for predicting tree mortality with mechanistic  
27 387 models. For conifers, higher  $RWC_{Stem}$  and lower EL values were related to a higher capacity to survive  
28 388 drought. However, this was not the case for angiosperms for which no physiological traits were  
29 389 identified as a potential proxy for the capacity of plant to recover although a similar pattern as to the one  
30 390 observed for the conifer species was identified.

## 37 391 **Author contributions**

38 392 MM and JMTR conceived and designed the experiment. MM and PEMS were responsible for  
39 393 running the measurements and carried out the data analysis. EB supervised the setting up of the micro-  
40 394 CT scans. MM, PEMS, HC and JMTR interpreted the results. MM wrote the first manuscript draft.  
41 395 JMTR, PEMS, HC and EB assisted substantially with manuscript development.

## 46 396 **Acknowledgement**

47 397 The authors thank Pierre Conchon and Julien Cartailier for their technical assistance, and the  
48 398 PIAF Research Unit staff for their support during this experiment. This research was funded by the  
49 399 project *ANR-18-CE20-0005 Hydrauleaks*.

## 54 400 **Data availability statement**

55 401 The data are not publicly available due to privacy restrictions.

56 402

403

For Peer Review

- 1
- 2
- 3
- 4
- 5
- 6
- 7
- 8
- 9
- 10
- 11
- 12
- 13
- 14
- 15
- 16
- 17
- 18
- 19
- 20
- 21
- 22
- 23
- 24
- 25
- 26
- 27
- 28
- 29
- 30
- 31
- 32
- 33
- 34
- 35
- 36
- 37
- 38
- 39
- 40
- 41
- 42
- 43
- 44
- 45
- 46
- 47
- 48
- 49
- 50
- 51
- 52
- 53
- 54
- 55
- 56
- 57
- 58
- 59
- 60



405 **References**

- 406 Adams HD, Zeppel MJB, Anderegg WRL, Hartmann H, Landhäusser SM, Tissue DT, Huxman TE,  
407 Hudson PJ, Franz TE, Allen CD, Anderegg LDL, Barron-Gafford GA, Beerling DJ, Breshears DD,  
408 Brodrribb TJ, Bugmann H, Cobb RC, Collins AD, Dickman LT, Duan H, Ewers BE, Galiano L,  
409 Galvez DA, Garcia-Forner N, Gaylord ML, Germino MJ, Gessler A, Hacke UG, Hakamada R,  
410 Hector A, Jenkins MW, Kane JM, Kolb TE, Law DJ, Lewis JD, Limousin JM, Love DM, Macalady  
411 AK, Martínez-Vilalta J, Mencuccini M, Mitchell PJ, Muss JD, O'Brien MJ, O'Grady AP, Pangle  
412 RE, Pinkard EA, Piper FI, Plaut JA, Pockman WT, Quirk J, Reinhardt K, Ripullone F, Ryan MG,  
413 Sala A, Sevanto S, Sperry JS, Vargas R, Vennetier M, Way DA, Xu C, Yopez EA, McDowell NG  
414 (2017) A multi-species synthesis of physiological mechanisms in drought-induced tree mortality.  
415 *Nat Ecol Evol* 1:1285–1291. <http://dx.doi.org/10.1038/s41559-017-0248-x>
- 416 Allen CD, Macalady AK, Chenchouni H, Bachelet D, McDowell N, Vennetier M, Kitzberger T, Rigling  
417 A, Breshears DD, Hogg EH (Ted., Gonzalez P, Fensham R, Zhang Z, Castro J, Demidova N, Lim  
418 JH, Allard G, Running SW, Semerci A, Cobb N (2010) A global overview of drought and heat-  
419 induced tree mortality reveals emerging climate change risks for forests. *For Ecol Manage*  
420 259:660–684.
- 421 Barigah TS, Charrier O, Douris M, Bonhomme M, Herbette S, Améglio T, Fichot R, Brignolas F,  
422 Cochard H (2013) Water stress-induced xylem hydraulic failure is a causal factor of tree mortality  
423 in beech and poplar. *Ann Bot* 112:1431–1437.
- 424 Barrs H., Weatherley PE (1962) A Re-Examination of the Relative Turgidity Techniques for Estimating  
425 Water Deficits in Leaves. *Aust J Biol Sci* 15:413–428.
- 426 Bartlett MK, Scaffoni C, Sack L (2012) The determinants of leaf turgor loss point and prediction of  
427 drought tolerance of species and biomes : a global meta-analysis. *Ecol Lett* 15:393–405.
- 428 Berry JA, Beerling DJ, Franks PJ (2010) Stomata: Key players in the earth system, past and present.  
429 *Curr Opin Plant Biol* 13:233–240. <http://dx.doi.org/10.1016/j.pbi.2010.04.013>
- 430 Bolte A, Czajkowski T, Coccozza C, Tognetti R, De Miguel M, Pšidová E, Ditmarová L, Dinca L, Delzon  
431 S, Cochard H, Ræbild A, De Luis M, Cvjetkovic B, Heiri C, Müller J (2016) Desiccation and  
432 mortality dynamics in seedlings of different European beech (*Fagus sylvatica* L.) populations  
433 under extreme drought conditions. *Front Plant Sci* 7:1–12.
- 434 Brodrribb TJ, Bowman DJMS, Nichols S, Delzon S, Burlett R (2010) Xylem function and growth rate  
435 interact to determine recovery rates after exposure to extreme water deficit. *New Phytol* 188:533–  
436 542.
- 437 Brodrribb TJ, Carriqui M, Delzon S, Lucani C (2017) Optical Measurement of Stem Xylem

- 1  
2  
3 438 Vulnerability. *Plant Physiol* 174:2054–2061.  
4  
5 439 Brodribb TJ, Cochard H (2009) Hydraulic Failure Defines the Recovery and Point of Death in Water-  
6  
7 440 Stressed Conifers. *Plant Physiol* 149:575–584.  
8  
9 441 <http://www.plantphysiol.org/cgi/doi/10.1104/pp.108.129783>  
10  
11 442 Brodribb TJ, Skelton RP, Mcadam SAM, Bienaimé D, Lucani CJ, Marmottant P (2016) Visual  
12  
13 443 quantification of embolism reveals leaf vulnerability to hydraulic failure. *New Phytol* 209:1403–  
14  
15 444 1409.  
16  
17 445 Buckley T (2005) The control of stomata by water balance. *New Phytol*:275–292.  
18  
19 446 Chaturvedi AK, Patel MK, Mishra A, Tiwari V, Jha B (2014) The SbMT-2 Gene from a Halophyte  
20  
21 447 Confers Abiotic Stress Tolerance and Modulates ROS Scavenging in Transgenic Tobacco. 9  
22  
23 448 Choat B, Badel E, Burllett R, Delzon S, Cochard H, Jansen S (2016) Noninvasive Measurement of  
24  
25 449 Vulnerability to Drought-Induced Embolism by X-Ray Microtomography. *Plant Physiol* 170:273–  
26  
27 450 282. <http://www.plantphysiol.org/lookup/doi/10.1104/pp.15.00732>  
28  
29 451 Choat B, Brodribb TJ, Brodersen CR, Duursma RA, López R, Medlyn BE (2018) Triggers of tree  
30  
31 452 mortality under drought. *Nature* 558:531–539. <https://doi.org/10.1038/s41586-018-0240-x>  
32  
33 453 Choat B, Jansen S, Brodribb TJ, Cochard H, Delzon S, Bhaskar R, Bucci SJ, Feild TS, Gleason SM,  
34  
35 454 Hacke UG, Jacobsen AL, Lens F, Maherali H, Martínez-Vilalta J, Mayr S, Mencuccini M, Mitchell  
36  
37 455 PJ, Nardini A, Pittermann J, Pratt RB, Sperry JS, Westoby M, Wright IJ, Zanne AE (2012) Global  
38  
39 456 convergence in the vulnerability of forests to drought. *Nature* 491:752–755.  
40  
41 457 Cochard H (1992) Vulnerability of several conifers to air embolism. *Tree Physiol* 11:73–83.  
42  
43 458 Cochard H (2002) A technique for measuring xylem hydraulic conductance under high negative  
44  
45 459 pressures. *Plant, Cell Environ* 25:815–819.  
46  
47 460 Cochard H, Badel E, Herbette S, Delzon S, Choat B, Jansen S (2013) Methods for measuring plant  
48  
49 461 vulnerability to cavitation: A critical review. *J Exp Bot* 64:4779–4791.  
50  
51 462 Cochard H, Delzon S, Badel E (2015) X-ray microtomography (micro-CT): A reference technology for  
52  
53 463 high-resolution quantification of xylem embolism in trees. *Plant, Cell Environ* 38:201–206.  
54  
55 464 Cochard H, Herbette S, Hernández E, Hölttä T, Mencuccini M (2009) The effects of sap ionic  
56  
57 465 composition on xylem vulnerability to cavitation. *J Exp Bot* 61:275–285.  
58  
59 466 Creek D, Lamarque LJ, Torres-Ruiz JM, Parise C, Burllett R, Tissue DT, Delzon S (2020) Xylem  
60  
467 embolism in leaves does not occur with open stomata: evidence from direct observations using the  
468 optical visualization technique. *J Exp Bot* 71:1151–1159.

- 1  
2  
3 469 Delzon S, Cochard H (2014) Recent advances in tree hydraulics highlight the ecological significance of  
4 470 the hydraulic safety margin. *New Phytol* 203:355–358.
- 6  
7 471 Delzon S, Douthe C, Sala A, Cochard H (2010) Mechanism of water-stress induced cavitation in  
8 472 conifers: Bordered pit structure and function support the hypothesis of seal capillary-seeding.  
9 473 *Plant, Cell Environ* 33:2101–2111.
- 12 474 Duan H, Duursma RA, Huang G, Smith RA, Choat B, O’Grady AP, Tissue DT (2014) Elevated [CO<sub>2</sub>]  
13 475 does not ameliorate the negative effects of elevated temperature on drought-induced mortality in  
14 476 *Eucalyptus radiata* seedlings. *Plant, Cell Environ* 37:1598–1613.
- 18 477 Epila J, De Baerdemaeker NJF, Vergeynst LL, Maes WH, Beeckman H, Steppe K (2017) Capacitive  
19 478 water release and internal leaf water relocation delay drought-induced cavitation in African  
20 479 *Maesopsis eminii*. *Tree Physiol* 37:481–490.
- 23 480 FAO (2006) Global forest resources assessment 2005—progress towards sustainable forest  
24 481 management. FAO For Pap 147
- 27 482 Guadagno CR, Ewers BE, Speckman HN, Aston TL, Huhn BJ, DeVore SB, Ladwig JT, Strawn RN,  
28 483 Weinig C (2017) Dead or alive? Using membrane failure and chlorophyll fluorescence to predict  
29 484 mortality from drought. *Plant Physiol* 175:pp.00581.2016.  
30 485 <http://www.plantphysiol.org/lookup/doi/10.1104/pp.16.00581>
- 34 486 Hacke UG, Venturas MD, Mackinnon ED, Jacobsen AL, Sperry JS, Pratt RB (2015) The standard  
35 487 centrifuge method accurately measures vulnerability curves of long-vesselled olive stems. *New*  
36 488 *Phytol* 205:116–127.
- 39 489 Hammond WM, Yu KL, Wilson LA, Will RE, Anderegg WRL, Adams HD (2019) Dead or dying?  
40 490 Quantifying the point of no return from hydraulic failure in drought-induced tree mortality. *New*  
41 491 *Phytol:nph.15922*. <https://onlinelibrary.wiley.com/doi/abs/10.1111/nph.15922>
- 44 492 Hogg EH, Hurdle PA (1997) Sap flow in trembling aspen implications for stomatal responses to VPD.  
45 493 *Tree Physiol* 17:501–509.
- 48 494 Holbrook NM (1995) Stem Water Storage. *Plant Stems*:151–174.
- 51 495 Hosking GP, Hutcheson JA (1988) Mountain beech (*Nothofagus solandri* var. *cliffortioides*) decline in  
52 496 the Kaweka range, north island, New Zealand. *New Zeal J Bot* 26:393–400.
- 54 497 Intergovernmental Panel on Climate Change (2014) Climate Change 2014: Synthesis Report; Chapter  
55 498 Observed Changes and their Causes.
- 58 499 Keenan TF, Hollinger DY, Bohrer G, Dragoni D, Munger JW, Schmid HP, Richardson AD (2013)  
59 500 Increase in forest water-use efficiency as atmospheric carbon dioxide concentrations rise. *Nature*

- 1  
2  
3 501 499:324–327.  
4  
5 502 King M., Ludford PM (1983) Chilling injury and electrolyte leakage in fruit of different tomato cultivars.  
6  
7 503 J Am Soc Hort Sci 108:74–77.  
8  
9 504 Klimešová J, Nobis MP, Herben T (2015) Senescence, ageing and death of the whole plant:  
10  
11 505 Morphological prerequisites and constraints of plant immortality. *New Phytol* 206:14–18.  
12  
13 506 Körner C (2019) No need for pipes when the well is dry - a comment on hydraulic failure in trees. *Tree*  
14  
15 507 *Physiol.* [https://academic.oup.com/treephys/advance-](https://academic.oup.com/treephys/advance-article/doi/10.1093/treephys/tpz030/5425286)  
16  
17 508 [article/doi/10.1093/treephys/tpz030/5425286](https://academic.oup.com/treephys/advance-article/doi/10.1093/treephys/tpz030/5425286)  
18  
19 509 Lamacque L, Charrier G, dos Santos Farnese F, Lemaire B, Ameglio T, Herbette S (2020) Drought-  
20  
21 510 induced mortality: branch diameter variation reveals a point of no recovery in lavender species.  
22  
23 511 *Plant Physiol*:pp.00165.2020.  
24  
25 512 Landmann G, Dreyer E (2006) Impacts of drought and heat on forest. Synthesis of available knowledge,  
26  
27 513 with emphasis on the 2003 event in Europe. *Ann For Sci* 3 6:567–652.  
28  
29 514 Lwanga JS (2003) Localized tree mortality following the drought of 1999 at Ngogo, Kibale National  
30  
31 515 Park, Uganda. *Afr J Ecol* 41:194–196.  
32  
33 516 Martin-StPaul N, Delzon S, Cochard H (2017) Plant resistance to drought depends on timely stomatal  
34  
35 517 closure. *Ecol Lett* 20:1437–1447.  
36  
37 518 Martinez-Vilalta J, Anderegg WRL, Sapes G, Sala A (2019) Greater focus on water pools may improve  
38  
39 519 our ability to understand and anticipate drought-induced mortality in plants. *New Phytol*  
40  
41 520 McDowell N, Pockman WT, Allen CD, Breashears DD, Cobb N, Kolb T, Plaut J, Sperry J, West A,  
42  
43 521 Williams DG, Yezzer EA (2008) Mechanisms of plants survival and mortality during drought: why  
44  
45 522 do some plants survive while others succumb to drought? *New Phytol* 178:719–739.  
46  
47 523 Pammenter N., Vander Willigen C (1998) A mathematical and statistical analysis of the curves  
48  
49 524 illustrating vulnerability of xylem to cavitation. *Tree Physiol* 18:589–593.  
50  
51 525 Petrov V, Hille J, Mueller-Roeber B, Gechev TS (2015) ROS-mediated abiotic stress-induced  
52  
53 526 programmed cell death in plants. *Front Plant Sci* 6:1–16.  
54  
55 527 <http://journal.frontiersin.org/Article/10.3389/fpls.2015.00069/abstract>  
56  
57 528 Reichstein M, Bahn M, Ciais P, Frank D, Mahecha MD, Seneviratne SI, Zscheischler J, Beer C,  
58  
59 529 Buchmann N, Frank DC, Papale D, Rammig A, Smith P, Thonicke K, Van Der Velde M, Vicca S,  
60  
530 Walz A, Wattenbach M (2013) Climate extremes and the carbon cycle. *Nature* 500:287–295.  
531  
<http://dx.doi.org/10.1038/nature12350>

- 1  
2  
3 532 Sakes A, Van Wiel M Der, Henselmans PWJ, Van Leeuwen JL, Dodou D, Breedveld P (2016) Shooting  
4 533 mechanisms in nature: A systematic review. PLoS One 11  
5  
6  
7 534 Salmon Y, Torres-Ruiz JM, Poyatos R, Martinez-Vilalta J, Meir P, Cochard H, Mencuccini M (2015)  
8 535 Balancing the risks of hydraulic failure and carbon starvation: A twig scale analysis in declining  
9 536 Scots pine. *Plant Cell Environ* 38:2575–2588.  
10  
11  
12 537 Schindelin J, Arganda-Carreras I, Frise E, Kaynig V, Longair M, Pietzsch T, Preibisch S, Rueden C,  
13 538 Saalfeld S, Schmid B, Tinevez JY, White DJ, Hartenstein V, Eliceiri K, Tomancak P, Cardona A  
14 539 (2012) Fiji: An open-source platform for biological-image analysis. *Nat Methods* 9:676–682.  
15  
16  
17 540 Sperry JS, Love DM (2015) What plant hydraulics can tell us about responses to climate-change  
18 541 droughts. *New Phytol* 207:14–27.  
19  
20  
21 542 Sutinen M-L, Palta JP, Reich PB (1992) Seasonal differences in freezing stress resistance of needles of  
22 543 *Pinus nigra* and *Pinus resinosa*: evaluation of the electrolyte leakage method. *Tree Physiol* 11:241–  
23 544 254. <https://academic.oup.com/treephys/article-lookup/doi/10.1093/treephys/11.3.241> (1 April  
24 545 2019, date last accessed ).  
25  
26  
27  
28 546 Suzuki N, Koussevitzky S, Mittler R, Miller G (2012) ROS and redox signalling in the response of  
29 547 plants to abiotic stress. *Plant, Cell Environ* 35:259–270.  
30  
31  
32 548 Taiz L, Zeiger E (2006) *Plant Physiology*. In: Sinauer Associates I (ed) Fourth Ed. pp 46–47.  
33  
34 549 Thomas H (2013) Senescence, ageing and death of the whole plant. :696–711.  
35  
36  
37 550 Torres-Ruiz JM, Cochard H, Choat B, Jansen S, López R, Tomášková I, Padilla-Díaz CM, Badel E,  
38 551 Burlett R, King A, Lenoir N, Martin-StPaul NK, Delzon S (2017) Xylem resistance to embolism:  
39 552 presenting a simple diagnostic test for the open vessel artefact. *New Phytol* 215:489–499.  
40  
41  
42 553 Torres-Ruiz JM, Cochard H, Mayr S, Beikircher B, Diaz-Espejo A, Rodriguez-Dominguez CM, Badel  
43 554 E, Fernández JE (2014) Vulnerability to cavitation in *Olea europaea* current-year shoots: Further  
44 555 evidence of an open-vessel artifact associated with centrifuge and air-injection techniques. *Physiol*  
45 556 *Plant* 152:465–474.  
46  
47  
48  
49 557 Torres-Ruiz JM, Jansen S, Choat B, McElrone AJ, Cochard H, Brodribb TJ, Badel E, Burlett R, Bouche  
50 558 PS, Brodersen CR, Li S, Morris H, Delzon S (2015) Direct X-Ray Microtomography Observation  
51 559 Confirms the Induction of Embolism upon Xylem Cutting under Tension. *Plant Physiol* 167:40–  
52 560 43. <http://www.plantphysiol.org/lookup/doi/10.1104/pp.114.249706>  
53  
54  
55  
56 561 Trueba S, Pan R, Scoffoni C, John GP, Davis SD, Sack L (2019) Thresholds for leaf damage due to  
57 562 dehydration: declines of hydraulic function, stomatal conductance and cellular integrity precede  
58 563 those for photochemistry. *New Phytol* 223:134–149.  
59  
60

- 1  
2  
3 564 Trumbore S, Brando P, Hartmann H (2015) Forest health and global change. *Science* (80- ) 349:814–  
4 565 818.
- 6  
7 566 Tyree MT, Zimmermann MH (2002) *Xylem structure and the ascent of sap*. Springer, New York, NY.
- 9  
10 567 Urli M, Porté AJ, Cochard H, Guengant Y, Burllett R, Delzon S (2013) Xylem embolism threshold for  
11 568 catastrophic hydraulic failure in angiosperm trees. *Tree Physiol* 33:672–683.
- 13  
14 569 Vandegheuchte MW, Guyot A, Hubau M, De Groote SRE, De Baerdemaeker NJF, Hayes M, Welte N,  
15 570 Lovelock CE, Lockington DA, Steppe K (2014) Long-term versus daily stem diameter variation  
16 571 in co-occurring mangrove species: Environmental versus ecophysiological drivers. *Agric For*  
17 572 *Meteorol* 192–193:51–58. <http://dx.doi.org/10.1016/j.agrformet.2014.03.002>
- 20  
21 573 Vilagrosa A, Bellot J, Vallejo VR, Gil-Pelegrín E (2003) Cavitation, stomatal conductance, and leaf  
22 574 dieback in seedlings of two co-occurring Mediterranean shrubs during an intense drought. *J Exp*  
23 575 *Bot* 54:2015–2024.
- 25  
26 576 Vilagrosa A, Morales F, Abadía A, Bellot J, Cochard H, Gil-Pelegrín E (2010) Are symplast tolerance  
27 577 to intense drought conditions and xylem vulnerability to cavitation coordinated? An integrated  
28 578 analysis of photosynthetic, hydraulic and leaf level processes in two Mediterranean drought-  
29 579 resistant species. *Environ Exp Bot* 69:233–242.  
30 580 <http://dx.doi.org/10.1016/j.envexpbot.2010.04.013>
- 34  
35 581 Wang C-R, Yang A-F, Yue G-D, Gao Q, Yin H-Y, Zhang J-R (2008) Enhanced expression of  
36 582 phospholipase C 1 ( ZmPLC1 ) improves drought tolerance in transgenic maize. *Planta* 227:1127–  
37 583 1140.
- 39  
40 584 Wang M, Zheng Q, Shen Q, Guo S (2013) The critical role of potassium in plant stress response. *Int J*  
41 585 *Mol Sci* 14:7370–7390.
- 43  
44 586 Widholm J (1972) The use of FDA and phenosafranin for determining viability of cultured plant cells.  
45 587 *Stain Technol* 47:189–94.
- 47  
48 588 Zhang MIN, Willison JHM (1987) An improved conductivity method for the measurement of frost  
49 589 hardness. *Can J Bot* 65:710–715. <http://www.nrcresearchpress.com/doi/10.1139/b87-095> (1 April  
50 590 2019, date last accessed ).

## 591 **Supporting information**

592 Additional supporting information may be found online in the Supporting Information section at the end  
593 of the article:

594 **Table S1.** PLC evolution during the time-course of the experiment.

595 **Table S2.** Evolution of the stem relative water content ( $RWC_{Stem}$ ), leaf relative water content ( $RWC_{Leaf}$ )  
 596 and electrolytes leakage (EL) during the time-course of the experiment

597 **Table S3.** Evolution of the percentage of bark living cells (%BLC) during the time-course of the  
 598 experiment.

599 **Figure S1.** Validation of the  $\Psi_{stem}$  measurements recorded with psychrometer and compared to the  $\Psi_{stem}$   
 600 measurements carried out with the Scholander pressure chamber on previously bagged leaves.

601 **Figure S2.** Plants flushing new leaves after re-watering.

## 602 **Figures legends**

603 Figure 1. Vulnerability curves to cavitation for *P. lusitanica* stems and *P. menziesii* stems. Vulnerability  
 604 curve for *P. lusitanica* stems obtained on four different samples using the optical method (Brodrribb et  
 605 al. 2017). The  $P_{50}$  is evaluated at -6.07MPa while the  $P_{88}$  is evaluated at -8.94MPa. Vulnerability curve  
 606 for *P. menziesii* stems obtained on five different samples using the Cavitrone technique developed by  
 607 Cochard in 2002. The  $P_{50}$  is evaluated at -3.73MPa and  $P_{88}$  is evaluated at -5.34MPa. Red solid lines  
 608 represent the  $P_{50}$  while red dashed lines represent the confidence interval around  $P_{50}$  at 95%. Violet and  
 609 green rectangles correspond to the water potential values at which *P. lusitanica* and *P. menziesii* were  
 610 respectively irrigated.

611 Figure 2. Box plots representing the dispersions of percentage loss of conductance (PLC) values for A  
 612 *P. lusitanica* and B *P. menziesii* before water stress (control) and before re-watering for recovering (R)  
 613 and dead (D) trees measured with the Xyl'EM apparatus for *P. lusitanica* and X-ray micro-CT for *P.*  
 614 *menziesii*.

615 Figure 3. Dynamic of the stem diameter (solid line) and evolution of the water potential (points) during  
 616 the time-course of the experiment. Stem diameter dynamic (in  $\mu m$ ) was recorded by Linear Variable  
 617 Differential Transformer (LVDT) for both species while the water potential was measured punctually  
 618 using a Scholander pressure chamber for *P. lusitanica* individuals and continuously by psychrometers  
 619 for *P. menziesii* individuals. The light grey rectangles represent the period where water was withheld to  
 620 simulate an extreme drought event. The red line indicates the percentage loss of conductance (PLC)  
 621 value at which the plant was re-watered. Panels A and B show the recovery of individuals after re-  
 622 watering in terms of stem diameter while panels C and D show dead individuals.

623 Figure 4. Variation of Stem Relative Water Content ( $RWC_{Stem}$ ) (panels A and B), Leaf Relative Water  
 624 Content ( $RWC_{Leaf}$ ) (panels C and D), stem Electrolyte Leakage (EL) (panels E and F) for *P. lusitanica*  
 625 and *P. menziesii*. Measurements were performed on all individuals in control conditions (Control) and  
 626 after the drought event (i.e. before the rehydration of the plants for recovered and dead individuals).

1  
2  
3 627 Figure 5. Cross-sections of *P. lusitanica* (A and B) and *P. menziesii* (C and D) stems in control  
4 628 conditions. Cross-sections were stained using fluorescein diacetate (FDA) (60 $\mu$ m thick cross-section –  
5 629 1% solution) and microphotographs were taken using a bright light (A and C) and an inverted  
6 630 fluorescence microscope (YFP filter; B and D). Living cells (fluorescent spots) are located in the phloem  
7 631 and outer bark for both species.

8  
9  
10  
11 632 Figure 6. Percentage of bark living cells (%BLC) stained with FDA in stem cross-sections in *P.*  
12 633 *lusitanica* (panel A) and *P. menziesii* (panel B). “R” refers to recovering trees and “D” refers to dead  
13 634 trees.

14  
15  
16  
17 635 Table S1. Table summarizing the evolution of the PLC during the time-course of the experiment in A  
18 636 *P. lusitanica* and B *P. menziesii*. Control values represent the mean value of the measurements  
19 637 performed before the drought event. BRW represents the measurements performed on the individuals  
20 638 the day of the rehydration.

21  
22  
23  
24 639 Table S2. Table summarizing the evolution of the stem relative water content (RWC<sub>Stem</sub>), leaf relative  
25 640 water content (RWC<sub>Leaf</sub>) and electrolytes leakage (EL) during the time-course of the experiment in A *P.*  
26 641 *lusitanica* and B *P. menziesii*. Control values represent the mean value of the measurements performed  
27 642 before the drought event. BRW represents the measurements performed on the individuals the day of  
28 643 the rehydration.

29  
30  
31  
32 644 Table S3. Table summarizing the evolution of the percentage of bark living cells (%BLC) during the  
33 645 time-course of the experiment in A *P. lusitanica* and B *P. menziesii*. Control values represent the mean  
34 646 value of the measurements performed before the drought event. BRW represents the measurements  
35 647 performed on the individuals the day of the rehydration.

36  
37  
38  
39 648 Figure S1. Validation of the stem water potential ( $\Psi_{\text{stem}}$ ) measurements recorded with psychrometer and  
40 649 compared to the  $\Psi_{\text{stem}}$  measurements carried out with the Scholander pressure chamber on previously  
41 650 bagged leaves. A for *P. lusitanica* and B for *P. menziesii*.

42  
43  
44  
45 651 Figure S2. Photographs of *P. lusitanica* plants flushing new leaves after experimenting a drought event  
46 652 and reaching levels of PLC of 98.6%. A 19 days after re-watering; B 28 days after re-watering.



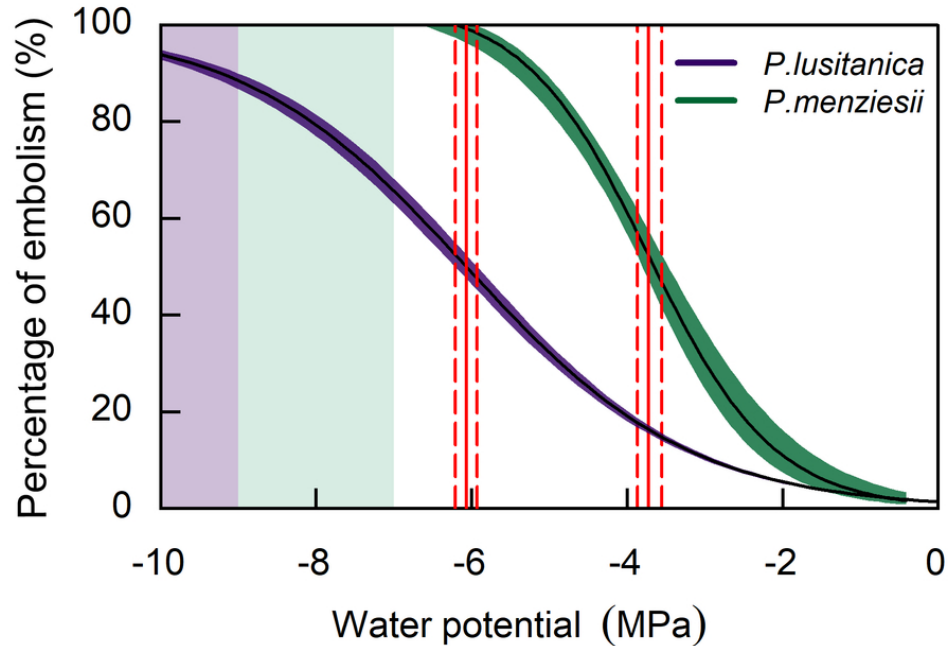
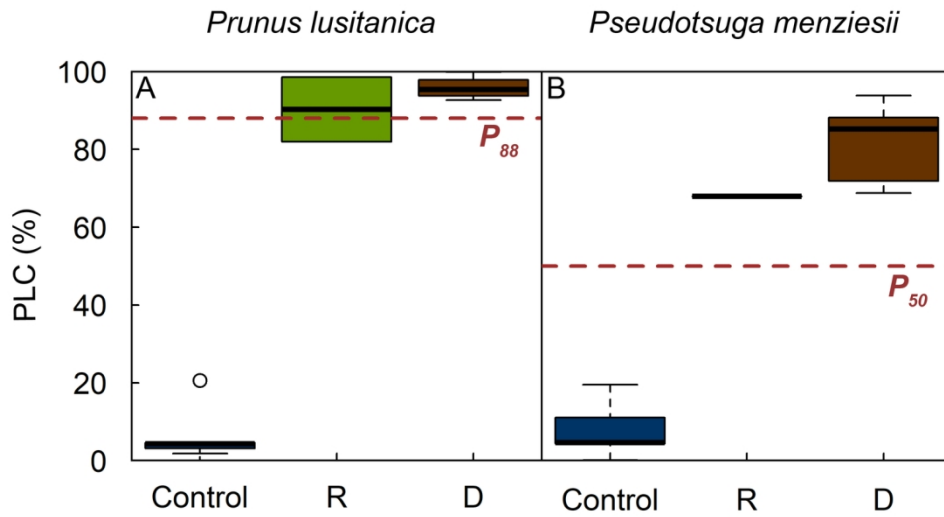


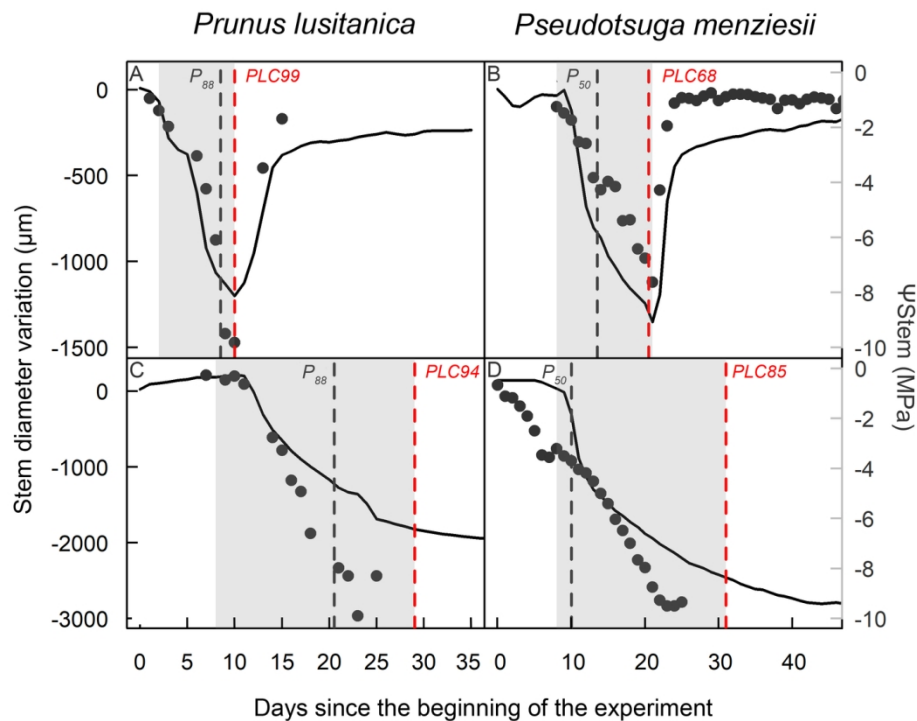
Figure 1. Vulnerability curves to cavitation for *Prunus lusitanica* L stems and *Pseudotsuga menziesii* M stems. Vulnerability curve for *P. lusitanica* stems obtained on four different samples using the optical method (Brodribb *et al.* 2017). The  $P_{50}$  is evaluated at -6.07MPa while the  $P_{88}$  is evaluated at -8.94MPa. Vulnerability curve for *P. menziesii* stems obtained on five different samples using the Cavitron technique developed by Cochard in 2002. The  $P_{50}$  is evaluated at -3.73MPa and  $P_{88}$  is evaluated at -5.34MPa. Red solid lines represent the  $P_{50}$  while red dashed lines represent the confidence interval around  $P_{50}$  at 95%. Violet and green rectangle correspond to the water potential values at which *P. lusitanica* and *P. menziesii* were respectively irrigated.

79x59mm (300 x 300 DPI)



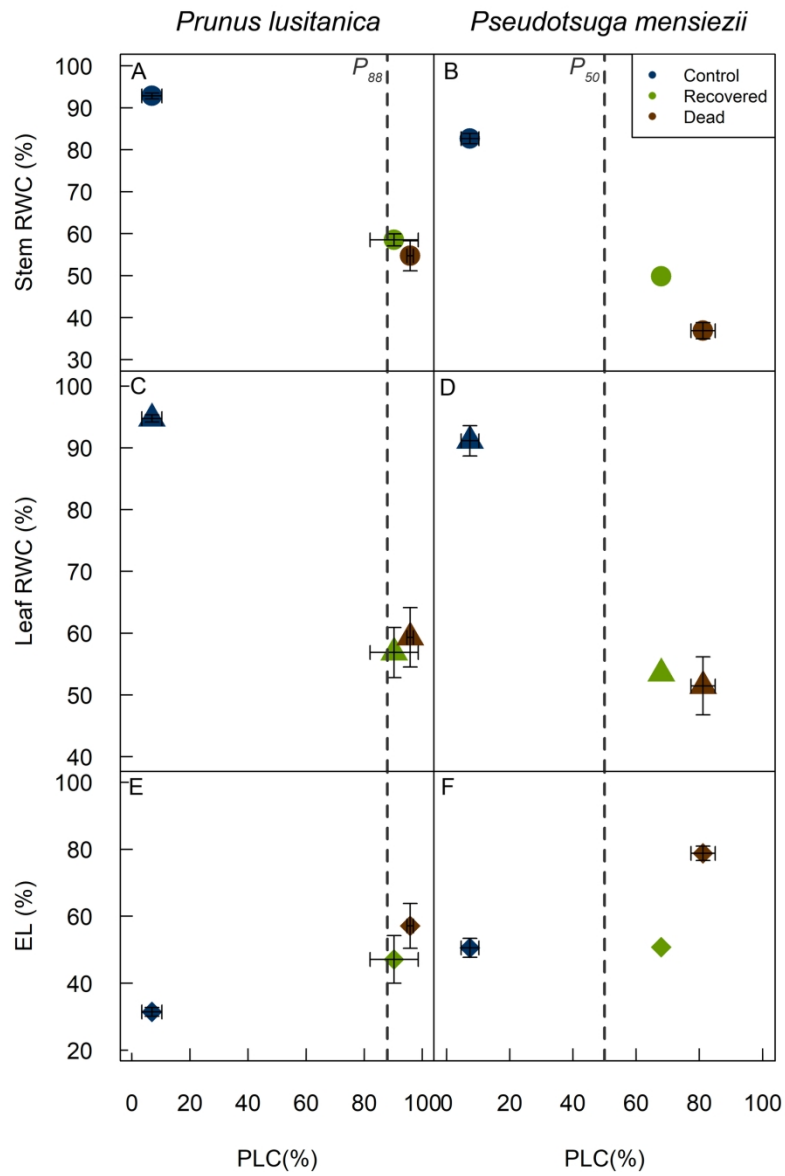
Box plots represents the dispersions of percentage loss of conductance (PLC) values for **A** *Prunus lusitanica*, **L** and **B** *Pseudotsuga menziesii*. M before water stress (control) and before re-watering for recovering (R) and dead (D) trees measured with the Xyl'em apparatus for *P. lusitanica* and X-ray micro-CT for *P. menziesii*.

140x79mm (300 x 300 DPI)



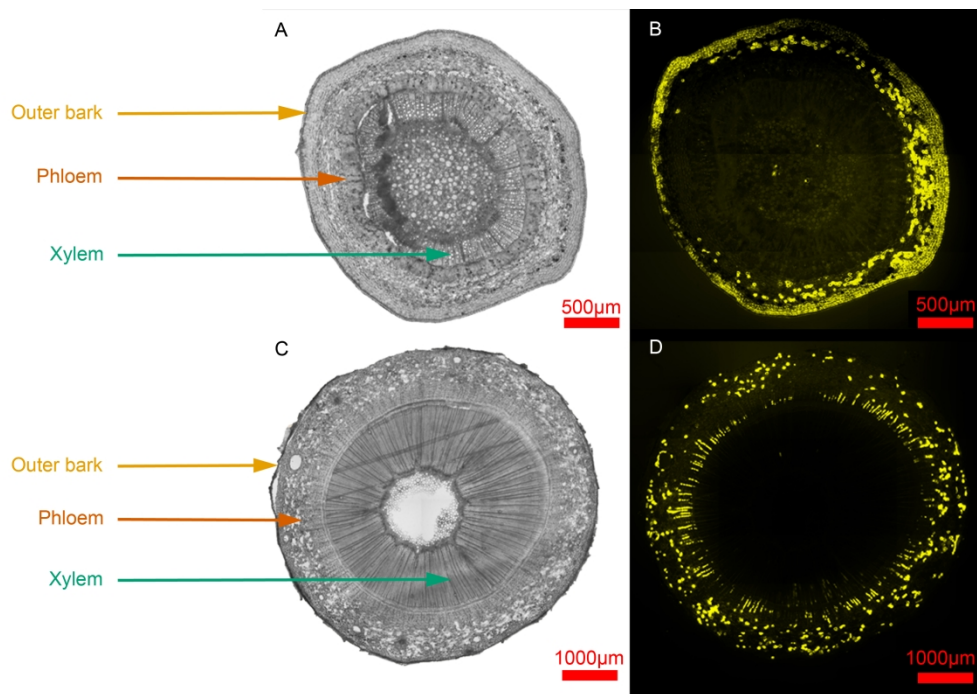
Dynamic of the stem diameter (solid line) and evolution of the water potential (points) during the time-course of the experiment. Stem diameter dynamic (in  $\mu\text{m}$ ) was recorded by LVDT for both species while the water potential was measured punctually using a Scholander pressure chamber for *Prunus lusitanica* individuals and continuously by psychrometers for *Pseudotsuga menziesii* individuals. The light grey rectangles represent the period where water was withheld to simulate an extreme drought event. Panels **A** and **B** show the recovery of individuals after re-watering in terms of stem diameter while panels **C** and **D** show dead individuals.

132x99mm (300 x 300 DPI)

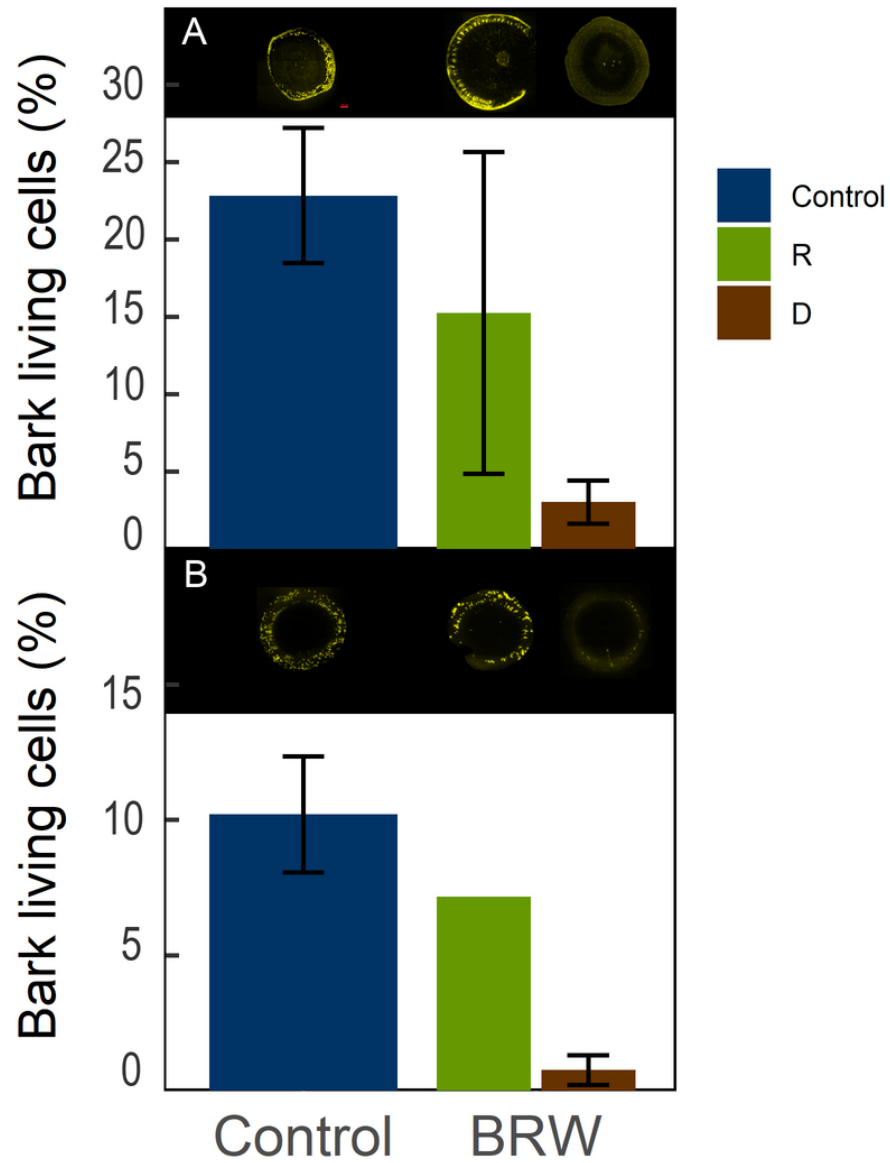


Variation of Stem Relative Water Content ( $RWC_{Stem}$ ) (panels **A** and **B**), Leaf Relative Water Content ( $RWC_{Leaf}$ ) (panels **C** and **D**), stem Electrolyte Leakage (EL) (panels **E** and **F**) for *Prunus lusitanica* L and *Pseudotsuga menziesii* M. Measurements were performed on all individuals in control conditions (Control) and after the drought event (e.g. before the rehydration of the plants for recovered and dead individuals).

165x219mm (300 x 300 DPI)



Cross sections of *Prunus lusitanica* L (A and B) and *Pseudotsuga menziesii* M (C and D) stems in control conditions. Cross sections were stained using fluorescein diacetate (FDA) (60µm thick cross section – 1% solution) and microphotographs were taken using a bright light (A and C) and an inverted fluorescence microscope (YFP filter B and D). Living cells (fluorescent spots) are located in the phloem and outer bark for both species.



Percentage of bark living cells (%BLC) stained with FDA in stem cross section in *Prunus lusitanica* L (panel **A**) and *Pseudotsuga menziesii* M (panel **B**). "R" refers to recovering trees and "D" refers to dead trees.

68x90mm (300 x 300 DPI)